World Conference on Timber Engineering Oslo 2023

PUSH-OUT TESTS OF WET-PROCESS ADHESIVE-BONDED BEECH TIMBER-CONCRETE AND TIMBER-POLYMER-CONCRETE COMPOSITE CONNECTIONS

Matthias Füchslin[1,2], Philippe Grönquist[1,3,4]*, Sandro Stucki[5,6], Tim Mamie[7], Steffen Kelch[7], Ingo Burgert[5,6], Andrea Frangi[1]

ABSTRACT: For timber-concrete composite (TCC) elements, a stiff and rigid connection results in an enhanced shear stress transfer at the timber-concrete interface, and thus, reduces the necessary cross-section height. A full composite action can hypothetically be achieved using an adhesive connection. In this study, an adhesive system developed for a wet-process gluing of concrete to European beech glued-laminated timber (GLT) is investigated by means of push-out tests. The tests were conducted on a specimen series with three different sizes of varying shear length, and evaluated using digital image correlation (DIC). The bondline shear strengths showed a pronounced size dependency, while the connection stiffness remained similar but showed a very large variability. These findings challenge the interpretation of bondline connection properties derived from push-out tests of glued TCC elements. In addition to the wet-process adhesive system with cement-based concrete, bonding between timber and a polymer concrete was investigated as an alternative possibility for TCC.

KEYWORDS: Adhesive connection, Digital image correlation, Polymer concrete, European beech GLT

1 INTRODUCTION

For the design of timber concrete-composite (TCC) structures, reliable knowledge of the specific connection behaviour is important. While annex B of Eurocode 5 [1] provides the "γ-method" in order to approximate the composite's flexural rigidity, the value of γ itself is to be derived from the connection stiffness K, which in turn, is to be determined for each specific type of connection. For the determination of K, usually, one of two types of push-out tests is commonly used: (1) a symmetric double-shear push-out test, such as suggested in annex C of CEN/TS 19103 [2], or (2) a single-shear push-out test with asymmetrical samples. Both methods possess specific advantages and disadvantages, such as potential prevailing asymmetry due to variability in timber material properties in test (1) when both side parts are timber, or high friction forces between timber and concrete for test (2). Additionally, in both tests, due to the load path, moments are induced and the resulting stress state does not reflect pure shear. Nonetheless, both methods tend to result in reliable values of K for most of the available TCC connection types, i.e., prevalently for the different metallic fastener and notch types.

To maximize composite action, and thus maximize the static efficiency of the TCC cross-section, a glued connection can be used. In this case, for the design of slabs, a value of $\gamma = 1$ (fully rigid connection) is usually assumed without the need for more precise analysis of K [3,4]. In fact, a handful of previous studies analysed the load-bearing behaviour of adhesively bonded TCC using building component scale sized push-out tests [5-13]. In most of the cases, the push-out tests were solely used for the purpose of verification of the load bearing capacity of the adhesive bond, whereas the connection stiffness K was not investigated. An exception is the study by Tannert et al. [13] who reported $K \approx 1'160 - 1'340$ kN/mm for a two-component epoxy adhesive (*Sikadur-32 Hi-Mod*). However, the aforementioned drawbacks of the testing methods do not necessarily permit to derive reliable values of K and of the shear strength, especially in the case of a glued connection, due to the non-local but dispersed and complex force flow.

In this study, European beech glued-laminated timber (GLT) was bonded in a wet process to self-compacting concrete using a newly developed hybrid adhesive combining epoxy and silane-terminated polymers. In order to assess a size-dependency of the connection properties, symmetric double-shear push-out tests were conducted on three specimen series with different shear length each. Surface strain fields were measured using digital image correlation (DIC), and bondline connection stiffness K was determined from surface displacement fields. In addition, two specimen series using a directly-bonding polymer concrete were tested to provide a benchmark and assess the bonding behaviour of polymer concrete on beech timber.

2 MATERIALS AND METHODS

2.1 Specimen series design

Three pushout specimen series with different shearing lengths were designed. In the case of the adhesive-bonded

[1] ETH Zurich, Institute of Structural Engineering, Switzerland
[2] B3 Kolb AG, Switzerland
[3] University of Stuttgart, Institute of Construction Materials, Germany
[4] University of Stuttgart, Materials Testing Institute, Germany
[5] Empa, Cellulose & Wood Materials, Switzerland
[6] ETH Zurich, Institute for Building Materials, Switzerland
[7] Sika Technology AG, Switzerland
* Correspondence: philippe.groenquist@iwb.uni-stuttgart.de

https://doi.org/10.52202/069179-0422

concrete in a wet process, the series were denoted as follows:

- **CL** (concrete large) with shearing length of 2 x 240 mm,
- **CM** (concrete medium) with shearing length of 2 x 180 mm, and
- **CS** (concrete small) with shearing length of 2 x 120 mm.

The shearing depth, and depth of all specimen components, was chosen as 240 mm. The detailed sample design is depicted in Figure 1. For series CL, CM, and CS, the predicted failure mode was a shear failure of the adhesive, while the probability of a shear failure of the concrete near the adhesive bond could not be entirely excluded. For the benchmark series using directly bonding polymer concrete, two series were chosen:

- **PM** (polymer concrete medium) with shear length of 180 mm, and
- **PS** (polymer concrete small) with shear length of 120 mm.

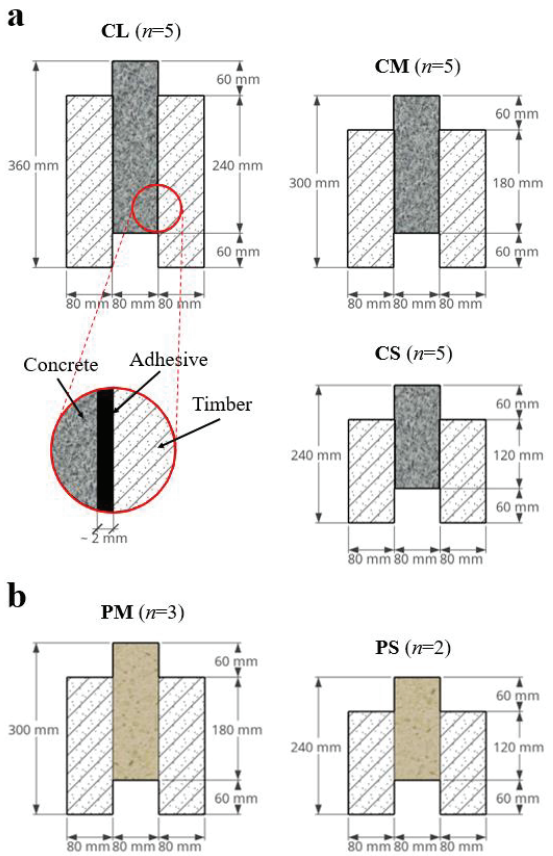

Figure 1: *Push-out specimen series with dimensions and number of tested specimens (n). Specimens have a constant depth of 240 mm (out of plane dimension).* ***a****: Series CL, CM, and CS for adhesively-bonded concrete in wet process.* ***b****: Series PM and PS for directly bonded polymer concrete.*

2.2 Specimen production

Defect-free GLT blocks of strength class GL48h were obtained from *Fagus Suisse SA*, made of European beech (*Fagus sylvatica*) wood of Swiss origin [14]. The blocks, were cut and planed to match the dimensions as shown in Figure 1. Their density was recorded as 722±20 kg/m^3, at an initial wood moisture content of approx. 8±0.5%. For the series CL, CM, and CS, for 5 specimens per series, a two-component silane-terminated polyurethane epoxy-hybrid (STP-E) adhesive, developed by *Sika Technology AG,* was evenly applied to both the timber side-parts of the pushout specimens. An amount of 1500 g/m^2 was applied on cleaned timber surfaces. After an initial phase of 25 minutes in horizontal position to allow for the adhesive to reach an optimal viscosity, see Figure 2a, the coated blocks were inserted into the formwork. *Sikacrete-16 SCC* [15], a self-compacting ready-mix concrete from *Sika Schweiz AG* of approx. grade C30/37 and maximal grain size of 16 mm, was cast in between the blocks, see Figure 2b. The specimens were left in the formwork for 5 days, and were tested after 28 days, meanwhile being covered by plastic foil during curing of the concrete to avoid drying.

For the series PM and PS, with 2 specimens each, the timber blocks were directly inserted into the formwork. *Sikadur 42 HE* [16], an epoxy-based grout from *Sika Schweiz AG*, in combination with quartz sand of grain size of < 4 mm, was cast. The specimens were left in the formwork for 5 days, and were tested after 28 days.

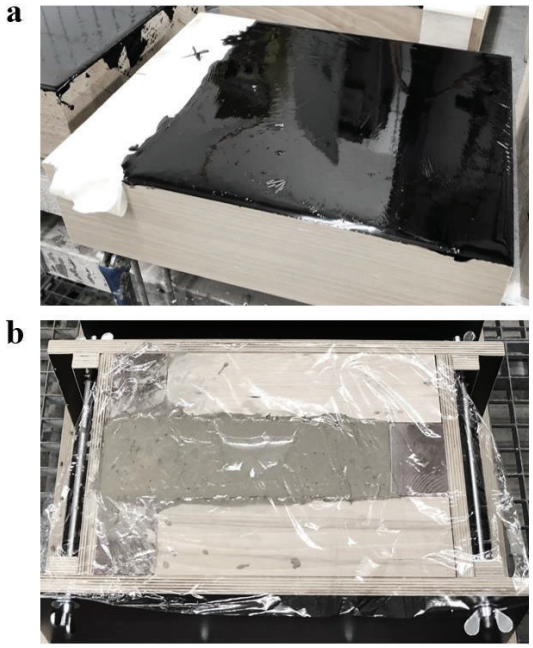

Figure 2: *Preparation of concrete specimens (CL, CM, CS).* ***a****: Application of controlled amount of STP-E adhesive (black).* ***b****: Casted self-compacting concrete mixture in formwork containing beech GLT with applied adhesive.*

2.3 Pushout testing

The specimens were tested using a displacement-controlled servo-hydraulic testing machine of type *Schenck 1600*, with a maximal capacity of 1600 kN (see Figure 3). Compressive forces were continuously recorded by a load cell. In addition to the machine displacement, redundant displacement measurements were conducted by three linear variable differential

transducers (LVDT) between the loading plates and surrounding the pushout specimens. Furthermore, a camera recorded an applied speckle pattern on the specimen sides in order to compute surface displacements and strain fields by means of digital image correlation (DIC). The specimens were initially loaded and unloaded twice until 30% of their estimated carrying capacity, and then ultimately loaded until failure.

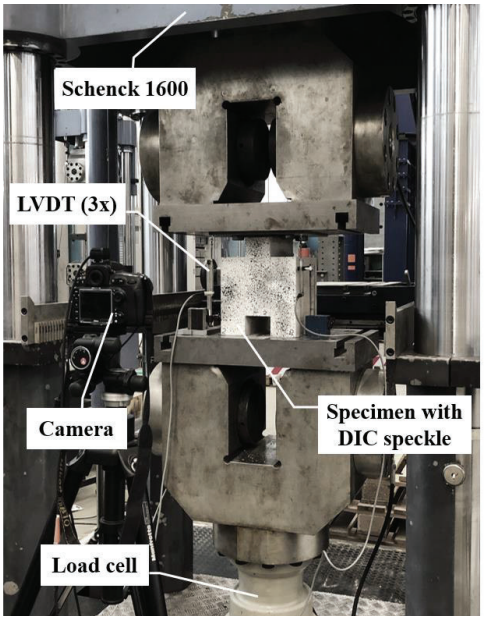

Figure 3: *Testing setup. Compressive Force applied by a displacement-controlled servo-hydraulic testing machine (Schenck 1600). Additional displacement measurements by three linear variable differential transducers (LVDT), and by digital image correlation (DIC).*

2.4 Determination of properties

The bondline shear strengths f_v were determined by dividing the maximum recorded forces F_{max} by the shearing area A_v:

$$f_v = \frac{F_{max}}{A_v}$$

The bondline connection stiffness K was determined for each of the two shearing lengths (right and left) per specimen separately, by dividing half of the applied force ΔF (force difference in a linear range of force-displacement) by the resulting average differential displacement between the timber and the concrete ($v_{m,t} - v_{m,c}$) parts:

$$K = \frac{\Delta F}{2(v_{m,t} - v_{m,c})}$$

The separate timber ($v_{m,t}$) and concrete ($v_{m,c}$) displacements were calculated locally for each of the parts near the bondline, but as averages over the whole shearing lengths, from computed displacement fields using the DIC technique. For DIC processing, *Ncorr*, an open source 2D DIC *Matlab*-based program was used [17].

3 RESULTS

Obtained results for shear strengths and bondline connection stiffnesses are shown in Figure 4 and Figure 5 as single data points, and summarized in Table 1 as mean values. An exemplary load vs. displacement curve is shown in Figure 6. A pronounced size-dependency in the shear-strengths across the different series CL (0.55 N/mm^2), CM (1.32 N/mm^2), and CS (2.22 N/mm^2) can be observed. However, these reported bondline shear strengths do not necessarily reflect the shear strength of the adhesive bond itself. As shown in Figure 7, the failure modes for the C-series (CL, CM, and CS) could be characterized as cohesive shear failure of the concrete near the bondline. For the same series, the connection stiffness shows no size-dependency, but instead, a very high scattering, as standard deviations surpass or are in the range of the mean values, see Table 1. Across all wet-process adhesive-bonded series, a mean value of 1.36 ± 0.72 N/mm^2 for the bondline strength at the moment of concrete cohesive failure at the bondline, and a mean value of 1'182 ± 1'469 kN/mm for the bondline connection stiffness can be reported.

The directly-bonded polymer concrete P-series (PM and PS) showed much better performances of the bondline, with overall mean values of 12.24 ± 3.34 N/mm^2 and 19'235 ± 25'202 kN/mm for the stress acting on the bondline at the moment of failure, and the bondline connection stiffness, respectively. Here, two failure modes were exclusively observed: Tensile-shear failure of polymer concrete and subsequent shear failure of timber, see Figure 7d. No size-dependency of the shear strengths is visible from the four tested specimens. However, an even higher standard deviation than for the adhesive-bonded specimens is reported for the bondline connection stiffness.

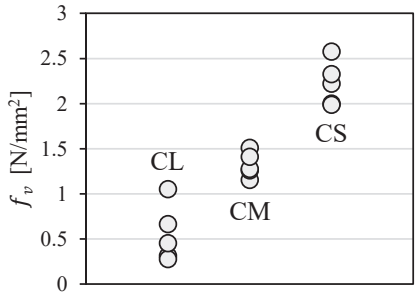

Figure 4: *Bondline shear strength (concrete cohesive failure) data points of series CL, CM, and CS, displaying size-dependency.*

https://doi.org/10.52202/069179-0422

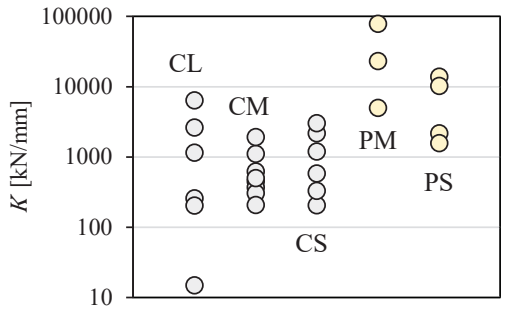

Figure 5: *Bondline connection stiffness (K) calculated from DIC data of both shearing lengths for each specimen of series CL, CM, CS, PM, and PS (note: Some data points missing due to DIC processing not possible).*

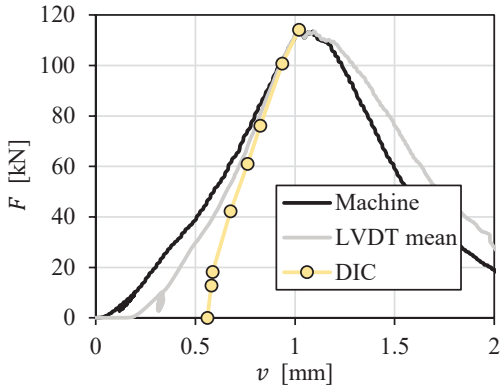

Figure 6: *Exemplary load (F) vs. displacement (v) curves of a specimen from series CS as measured by machine displacement, mean value of 3 LVDT curves, and displacement computed by DIC (markers represent images taken by camera). Curves were horizontally shifted to reach F_{max} simultaneously.*

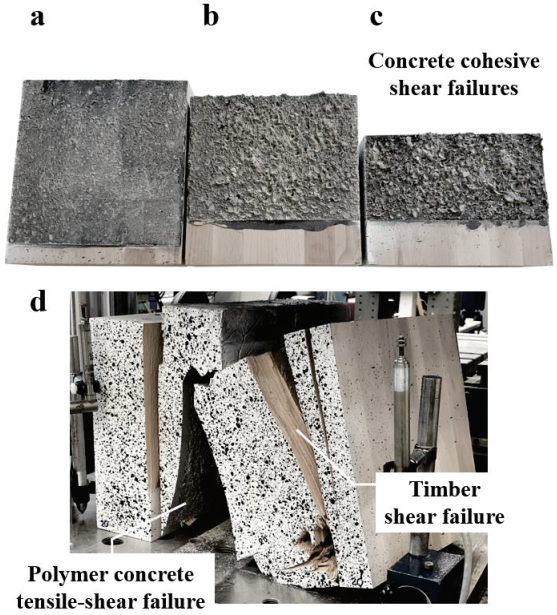

Figure 7: *Observed failure modes. a: Series CL: Concrete cohesive shear failure. b: Series CM: Concrete cohesive shear failure. b: Series CM: Concrete cohesive shear failure. d: Series PM and PS: Polymer concrete tensile-shear failure and timber shear failure.*

Table 1*: Results of push-out tests (mean values ± standard deviations of single series): n: Number of specimens, l_v: Shearing length, A_v: Shearing Area, F_{max}: Force at failure, f_v: Shear strength of bondline, K: Bondline connection stiffness calculated using DIC fields.*

	n	l_v[mm]	A_v[mm²]	F_{max} [kN]	f_v [N/mm²]	K [kN/mm]
CL	5	2 x 240	115'200	63.5 ± 32.8	0.55 ± 0.28[a]	1'175 ± 2'465
CM	5	2 x 180	86'400	114.1 ± 10.7	1.32 ± 0.12[a]	685 ± 569
CS	5	2 x 120	57'600	128.0 ± 12.7	2.22 ± 0.22[a]	1'253 ± 1'130
				ø:	1.36 ± 0.72[a]	1'182 ± 1'469
PM	2	2 x 180	86'400	1'025.0 ± 360.0	>[7.05; 14.26][b,c]	31'754 ± 30'554[d]
PS	2	2 x 120	57'600	795.9 ± 170.2	>[11.73; 15.91][b,c]	6'965 ± 6'064[d]
				ø:	>12.24 ± 3.34[b]	19'235 ± 25'202[d]

[a]: Shear stress acting on bondline at the moment of concrete cohesive failure at/near the adhesive bondline.

[b]: Shear stress acting on bondline at the moment of polymer concrete failure.

[c]: Data points of both tested specimens.

[d]: Interfacial zone stiffness (polymer concrete and timber), no observed bondline compliance (see Figure 10).

https://doi.org/10.52202/069179-0422

4 DISCUSSION

From the exemplary load displacement curves obtained by the three different methods (machine, LVDT, and DIC displacements) as shown in Figure 6, it can be seen that the measured DIC fields can be validated well by the LVDT measurements in regions of higher loads, after the curves are horizontally shifted to match at F_{max}. Therefore, justifying the use of DIC in order to calculate bondline stiffness values K. It can also be seen, that there is a pronounced stiffness difference between the three displacement-recording techniques, showing that both machine and LVDT displacements appear too compliant in comparison to DIC displacements, until ~70% of the maximal load.

Exemplary DIC fields are shown in Figure 8 for a specimen of series CS. From this data, it is clearly visible that for the C-series, a distinct bondline behaviour can be identified: The vertical displacements shown in Figure 8a differ significantly between concrete and timber, meaning that deformation happens primarily at the bondline. This is supported by the shear strains shown in Figure 8c, and in turn, supports the determination attempt of a bondline connection stiffness K in the case of wet-process adhesively-bonded pushout specimens, as presented in Table 1.

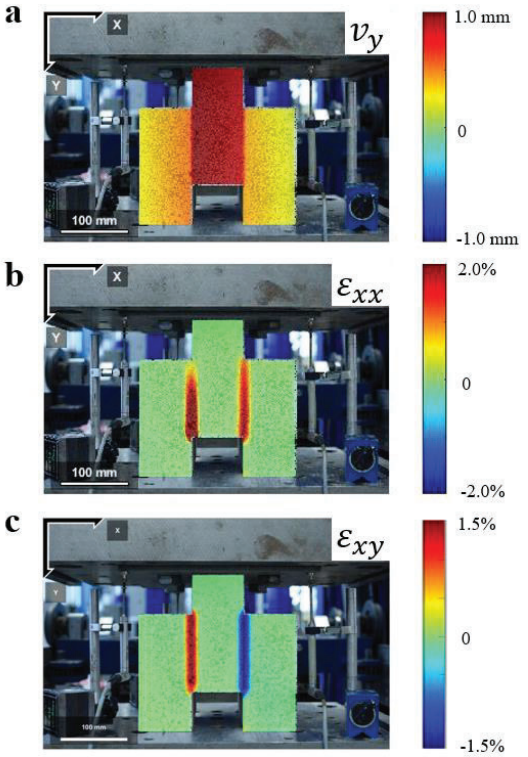

Figure 8: *Exemplary DIC analysis of a specimen of series CS at a force value close to failure of $F \approx F_{max}$ (133 kN).* ***a****: Vertical deformations (v_y), used for determination of bondline connection stiffness K.* ***b****: Horizontal strains (ε_{xx}).* ***c****: Shear strains (ε_{xy}).*

The observed size-dependency in the bondline shear strength may have been influenced by the superposition and interrelations of the following stresses acting at the bondline:

- Stresses induced by concrete shrinkage during hardening,
- possible stresses induced by timber swelling or shrinkage, caused by influences of the concrete water during hardening and subsequent testing hall climate,
- tensile stresses induced by the moment of eccentricity due to the load path inherent to the double-shear push-out setup ($\sigma_{ecc.} \propto b_t / l_v^2$, where b_t is the in-plane width of the timber side parts, and l_v is the shearing length).

These stresses tend to induce undesirable peeling stresses on the bondline, negatively influencing the obtained shear strengths. In addition, the fact these stresses, together with the main shear stresses from the vertical load, are typically shear-lag distributed over their respective shearing lengths, certainly affected the obtained values. In fact, size effects, supposedly stemming from such influences, are a well know phenomenon in testing of structural adhesives [18]. In standards where shear testing of adhesive bondlines with variable possible specimen sizes is possible, e.g. as in annex D of EN 14080 [19], corrections factors of shear strength are recommended for size deviations with respect to a reference size. However, in the present study and within its intents, it is not clear what specimen size could be considered as a suitable reference size.

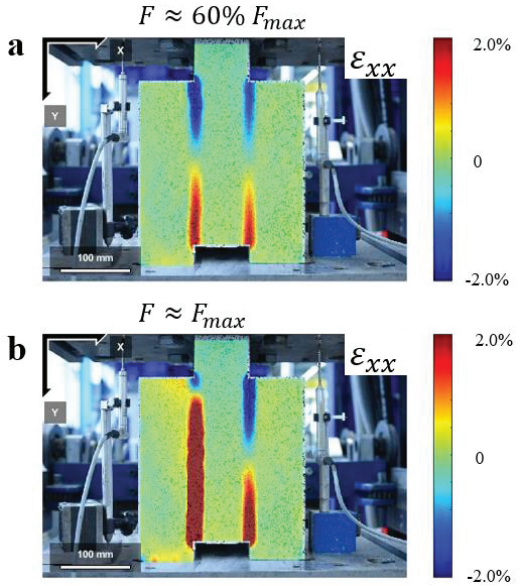

Figure 9: *Example of obtained horizontal strain (ε_{xx}) evolution for a specimen of series CL at two different load levels.* ***a****: At a force of $F \approx 60\%F_{max}$ (30 kN).* ***b****: At a force close to failure $F \approx F_{max}$ (51 kN).*

Moreover, additional influences such as friction at the bottom of the side timber parts between wood and metal plate, as well as slight but possible unevenness of the timber side parts may also have, and even to a greater extent, influenced the results. An example is shown in Figure 9: Here, the horizontal strain evolution at the bondline is shown for a specimen of series CL. While still

https://doi.org/10.52202/069179-0422

symmetrical at the lower load level, the horizontal strain is not symmetrical anymore across the two bondlines at the higher load level close to failure. In contrast, this behaviour could not be observed in the case of the CS specimen shown in Figure 8b. It is to be expected, that the horizontal stresses at the bondline highly affect the bondline performance, as e.g. they may directly reflect the amount of perpendicular tensile stress acting at the bondline. A symmetrical behaviour would a priori result in a better bondline performance.

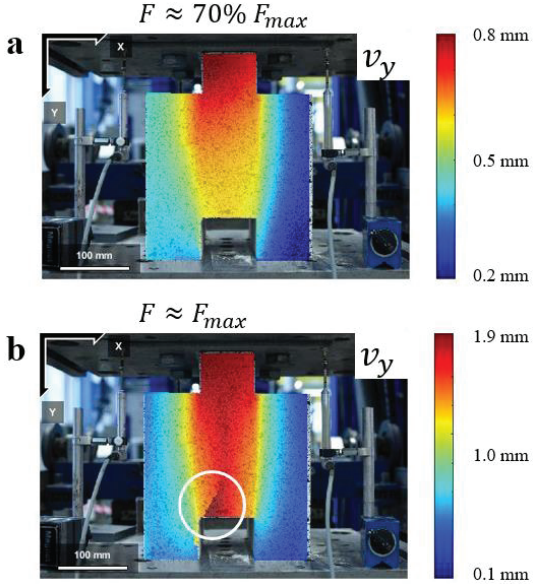

Figure 10: *Example of obtained vertical deformation ($\boldsymbol{v_y}$) evolution for a specimen of series PM at two different load levels used for determination of bondline connection stiffness K.* ***a****: At a force of $F \approx 70\%F_{max}$ (890 kN).* ***b****: At a force close to failure $F \approx F_{max}$ (1230 kN), white circle shows polymer concrete tensile-shear failure.*

Furthermore, an additional aspect with high potential impact is the production process of the specimens. As can be seen in studies at small scale [20,21], slight variability in adhesive pot or open time, or concrete mixture (e.g. water to cement ratio), may influence measured values. A hint towards the latter influence can be seen in the shear failure surfaces shown in Figure 7. A rather smooth shear failure was consistently observed for the samples CL, while more rough surfaces were observed for the series CM and CS, which cannot be explained otherwise. Herewith, the series CS, with the highest bondline strength, displayed the roughest surface, where the roughness appears to be characterized by the size of the concrete aggregates. It should also be noted, that in particular for a brittle material such as concrete, the concept of pure shear failure can be questioned, as the shear strength (or as in this case a cohesive shear strength at the bondline) is not the result of a pure shear stress state, but always involves tensile stresses. Therefore, the strength values provided in Table 1 should be interpreted accordingly, meaning that the shear strength of the adhesive connection itself could in theory be higher. The reported values rather represent the acting shear stresses in the bondline at the moment of cohesive concrete failure, which is, as said above, to be considered specific for this pushout tests situation. Therefore, the problematics and relevance of the observed size effect for design can safely be relativized.

From a bondline strength perspective, the P-series proved to significantly outperform the adhesive bond of the C-series. This is explained by the fact that polymer concrete, in contrast to cement-based concrete, possesses a rather high tensile (cohesive) strength. The herein reported overall mean value for the push-out strength of 12.24 N/mm^2, at the moment of polymer concrete failure, is slightly higher than comparable polymer concrete alternatives bonded to softwood and tested in a push-out manner [22,23].

While the high variability obtained for the bondline connection stiffness of the C-series can be attributed, as the variability in bondline strength, to the overall variability of load-deformation behaviour (caused by the above mentioned effects), this is not entirely the case for the P-series. Here, as can be seen from the vertical deformation exemplarily shown in Figure 10 for a PM specimen, a distinctive bondline deformation behaviour cannot be identified. Instead, the whole interface region appears to deform continuously, as the vertical deformations happen in the timber and in the polymer concrete. Therefore, the bondline stiffness values of Table 1 for PM and PS do not possess any physical meaning, and for design, $\gamma = 1$ can be assumed straightforwardly. Note that this is also the case for the wet-process adhesive-bonded C-series, since for most specimens $K \gtrsim 1'000$ kN/mm. However, and in contrast, the physical meaning of K can be supported by the DIC fields shown in Figure 8a.

Finally, while pushout tests assessed by DIC were certainly insightful in these cases of continuous rigid connections, they proved to produce values that are difficult to be fully understood and interpreted. Therefore, alternative or additional testing methods, e.g. bending tests, can be recommended in order to characterize adhesive bonds for TCC elements.

5 CONCLUSIONS

The study showed that in the case of adhesive-bonded TCC connections produced in wet process, results of push-out tests need to be interpreted and used with caution. Shear strengths were found to be strongly size-dependent, and do not directly reflect adhesion strength, but rather cohesive strength of concrete at the bondline. Furthermore, and even though DIC proved to be a powerful characterization tool, a reliable derivation of connection stiffness K was hardly possible. However, for most specimens, $K \gtrsim 1'000$ kN/mm could still be reported, justifying the prevalent assumption of $\gamma = 1$ in the case of a continuous adhesively-bonded TCC connection. Finally, an alternative to the classical adhesive bonding of cement-based concrete to beech wood was demonstrated in the form of directly-bonding polymer concrete. Here, pushout tests showed a far superior performance of the bondline compared to wet-process glued cement-based concrete.

ACKNOWLEDEGEMTS

We sincerely thank Thomas Schnider for the preparation of the casting formwork and Dominik Werne and Pius Herzog for help with the testing setup. Furthermore, we would like to express our gratitude to the further involved project partners from *Fagus Suisse SA* and *Sika Technology AG*. This project was funded by *Innosuisse - Swiss Innovation Agency* (37233.1 IP-ENG *'Verklebter Holz-Beton-Verbund - Mit Buchenholz und Polymerbeton zu innovativen Lösungen'*).

REFERENCES

[1] EN 1995-1-1:2004, Eurocode 5: Design of timber structures - Part 1-1: General - Common rules and rules for buildings.

[2] CEN/TS 19103:2021, Eurocode 5: Design of Timber Structures — Structural design of timber-concrete composite structures — Common rules and rules for buildings.

[3] Dias, A., Schänzlin J., Dietsch P.: Design of timber-concrete composite structures: A state-of-the-art report by COST Action FP1402 WG 4. Shaker Verlag, Aachen, 2018.

[4] Koch S., Grönquist P., Monney C., Burgert I., Frangi A.: Densified delignified wood as bio-based fiber reinforcement for stiffness increase of timber structures. Composites Part A, 163, 2022.

[5] Negrão J. H., Oliveira F. M., Oliveira C. L.: Investigation on Timber-Concrete Glued Composites. 9th World Conference on Timber Engineering (WCTE), Portland US, 2006.

[6] Brunner M., Romer M., Schnüriger M.: Timber-concrete-composite with an adhesive connector (wet on wet process). Materials and Structures, 40:119–126, 2007.

[7] Kanócz J., Bajzecerová V.: Timber - Concrete composite elements with various composite connections part 3: Adhesive connection. Wood Research, 60(6): 939-952, 2015.

[8] Eisenhut L., Seim W., Kühlborn S.: Adhesive-bonded timber-concrete composites – Experimental and numerical investigation of hygrothermal effects. Engineering Structures, 125, 2016.

[9] Kostić S., Meier S., Cabane E., Burgert I.: Enhancing the performance of beech-timber concrete hybrids by a wood surface pre-treatment using sol-gel chemistry. Heliyon, 4(9):e00762, 2018.

[10] Frohnmüller J., Fischer J., Seim W.: Full-scale testing of adhesively bonded timber-concrete composite beams. Materials and Structures, 54:187, 2021.

[11] Kästner M., Rautenstrauch K.: Polymermörtel-Klebverbindungen für Holz-Beton-Verbundbrücken Teil 1. Bautechnik, 98, 2021.

[12] Arendt S., Sutter M., Breidenbach M., Schlag R., Schmid V.: Neue Forschungsergebnisse zu Nass-in-Nass geklebten Holz-Beton-Verbunddecken. Bautechnik, 99, 2022.

[13] Tannert T., Gerber A., Vallee T.: Hybrid adhesively bonded timber-concrete-composite floors. International Journal of Adhesion and Adhesives, 97, 2020.

[14] Fagus Suisse SA. Fagus Stabschichtholz - Bemessungswerte für Buche. 2021.

[15] Sika Schweiz AG: Produktdatenblatt Sikacrete®-16 SCC. Version 01.05, July 2020.

[16] Sika Schweiz AG: Produktdatenblatt Sikadur®-42 HE. Version 02.04, August 2020.

[17] Blaber J., Adair B., Antoniou A.: Ncorr: Open-Source 2D Digital Image Correlation Matlab Software. Experimental Mechanics, 2015.

[18] Okkonen E. A., River B. H.: Factors affecting the strength of block-shear specimens. Forest Products Journal, 39(1), 1988.

[19] EN 14080:2013: Timber structures – Glued laminated timber and glued solid timber – Requirements.

[20] Fu Q., Yan L., Thielker N.A., Kasal B.: Effects of concrete type, concrete surface conditions and wood species on interfacial properties of adhesively-bonded timber – Concrete composite joints. International Journal of Adhesion & Adhesives, 107, 2021.

[21] Nemati Giv A., Fu Q., Yan L., Kasal B.: Interfacial bond strength of epoxy and PUR adhesively bonded timber-concrete composite joints manufactured in dry and wet processes. Construction and Building Materials, 311, 2021.

[22] Becker W., Schober K., Weber J.: Vergussknotenlösungen im Ingenieurholzbau. Bautechnik 93, 2016.

[23] Jahreis M.: Zur Entwicklung von Polymervergussknotenlösungen für den Holzbau. Dissertation, Bauhaus-Universität Weimar, 2019.

https://doi.org/10.52202/069179-0422